Original Research

Responses of Chemical Functional Groups in Coleus Blumei Roots under Lead Stress with Exogenous Selenium Treatment Using 2-dimensional Correlation FTIR Spectra

Mianhao Hu[1]*, Juhong Yuan[2]

[1] Institute of Ecological Economics, Jiangxi University of Finance and Economics, Nanchang, China
[2] Institute of Environment and Plant Science, Jiangxi University of Finance and Economics, Nanchang, China

Abstract

Changes of chemical compositions in *Coleus blumei* roots under lead (Pb) stress with different concentrations of selenium (Se) treatments (0, 0.1, 0.5, 1.0, 2.5, and 5.0 mM) were analyzed by Fourier transform infrared (FTIR) spectrometry and 2-dimensional FTIR correlation spectroscopy. This was to investigate the spectroscopy differences and microscopic dynamics of chemical functional groups in *C. blumei* roots under Pb stress with exogenous selenium treatment. The results show that the peak shapes remained basically unchanged in *C. blumei* roots exposed to Pb stress with different concentrations of Se treatments, and the wave number of the absorption peaks remained stationary. However, there was a significant difference in absorption peak strength, which is influenced by chemical composition. Semi-quantitative data indicate that there were obvious differences between the characteristics of the organic functional groups. There were differences between the 2D-FTIR correlation spectra of C. blumei roots in the region of 929-1,800 cm^{-1} under Pb stress with different concentrations of Se treatments, which are probably related to differences in chemical composition and structure. The FTIR spectra confirm the presence of various functional groups from the responses to abiotic stresses in the plant, and 2D-FTIR correlation spectroscopy may be a convenient and effective method in the study of plant molecular interactions under environmental stress.

Keywords: lead stress, exogenous selenium, Coleus blumei, 2-dimensional correlation FTIR spectra

Introduction

Lead (Pb), the most common heavy metal pollutant, has caused great concern as a result of its widespread occurrence, toxic nature, and long duration in biological systems [1]. It mainly originates from mining and smelting activities, Pb-containing paints, gasoline and explosives, cosmetics, storage batteries, fertilizers, herbicides, pesticides, and other industrial products [2-3], and from Pb-enriched municipal sewage sludge [4]. Though regulatory measures have been adopted

---
*e-mail: yankeu1@163.com

in many countries to control Pb input in the environment, it remains one of the most serious global environmental and human hazards [2]. With rapid developments in industry globally, many potential Pb sources are indispensable for modern human life, so soil pollution with Pb is not likely to be reduced in the near future [2]. These lead-cycles caused by anthropogenic sources are much more extended than the natural lead-cycle, and so it can accumulate in individual organisms, with subsequent accumulation along the entire food chain, which is a potential threat to human health [5]. Due to extensive use, their increased levels in the environment may lead to serious concerns for the environment and the global population.

In recent years, bioremediation has provided an alternative tool to destroy or render Pb contaminants non-toxic through biological activity. This method is cost effective, but Pb also causes plant injury [6]. Thus, plant response to Pb contamination is still a key problem, and a concerted effort is being made to find factors that influence the decrease of Pb absorption or toxicity in plants. Selenium (Se) plays an important role in conferring tolerance to Pb stresses in plants. Low concentrations of Se can improve cell viability in Pb-treated plants [7]. However, the beneficial effects of higher concentrations of Se could be related to the reduction of lipid peroxidation and cell membrane injury [7-8]. The antagonistic effects of Se on the Pb-stressed plants were found to heavily depend on the Se dose in the nutrient solution [8]. Therefore, Se may be a useful tool for minimizing the toxic effects of lead toxicity through its potent antioxidant activity [9]. Some studies have also shown that selenium mitigation of Pb accumulation in plants could decrease the Pb bioavailability in soil [10-11]. The beneficial effects of Se on plants exposed to Pb, and the possible mechanisms of the Se-enhanced resistance of plants to Pb toxicity, have been reported over a narrow range of concentrations. However, these mechanisms for Se-mediated detoxification of Pb have only involved the antioxidative stress response, so the mechanisms by which Se counteracts stress have not been fully clarified, and further research is necessary.

Two-dimensional correlation Fourier transform infrared FTIR spectroscopy (2D-FTIR) is a relatively new spectroscopic technique. It has been widely used to analyze spectral signals that change as functions of time, as well as other physical variables such as temperature, pressure, and concentration [12]. It can be useful for extracting more information from the chemical spectra, and elucidating the dynamic changes of functional groups, and the intramolecular and intermolecular interaction exposure to different conditions [13]. Biomolecules (proteins, polysaccharides, and in some instances lignin and other phenolic compounds) confer the ability to bind heavy metals non-covalently and/or covalently via functional groups [14], resulting in an enhanced stabilization ability of heavy metals in the plant [15]. However, the binding ability depends on the amount of various functional groups in the plant, such as hydroxyl,

carboxyl, and carbonyl groups [16], and is important for a long-term heavy metal stabilization strategy in the plant or contaminated soils [15]. Previous research has shown that appropriate Se supplementation may ameliorate Pb-induced oxidative stress by decreasing lipid peroxidation and altering the antioxidant defense system [17]. However, the possible interaction mechanism of organic molecules constitutes a variety of functional groups, and the chemical composition of the coleus plant is not yet fully understood. Therefore, the major objective of the present study was to investigate the functional group changes in *Coleus blumei* roots under Pb stress with the exogenous application of Se using FTIR and 2D-FTIR. We hoped to understand the molecular structure differences of Se-mediated detoxification, and to provide a new perspective on the unique role of Se in counteracting the negative effects of various environmental stresses in plants.

Materials and Methods

Plant Pre-Treatment and Experimental Design

Coleus (*Coleus blumei* benth.) used in this study was from the clone continually propagated in the Botanical Garden, Nanchang, Jiangxi, China. The plants were washed with tap water to allow them to adapt to a water environment. After one month, these plants were transferred to 2.5 L pots (16 plants per pot) containing 1/4 strength Hoagland nutrient solution (HNS) [18]. Plants were acclimatized in the hydroponic system for 2 weeks. Experiments were carried out using the simplest hydroponic system, i.e., a water culture system with slight modifications (modified Hoagland nutrient solution, MHNS) [19]. The platform that contained the plants was made of Styrofoam and floated directly on the nutrient solution. Air was bubbled through the nutrient solution using an air pump connected to an air stone to supply oxygen to the roots of the plants. The experiment was set up as a completely randomized design with 7 treatments each and 4 replications. Based on preliminary experiments, the acclimated plants were transferred to the full-strength MHNS, which had 1.0 mM lead (Pb) in the form of $Pb(NO_3)_2$ (Sigma-Aldrich, St. Louis, MO, USA), and then different concentrations of sodium selenite (Na_2SeO_3; Sigma) (0, 0.1, 0.5, 1.0, 2.5, and 5.0 mM) were added. These treatments were denoted as Pb1.0Se0, Pb1.0Se0.1, Pb1.0Se0.5, Pb1.0Se1.0, Pb1.0Se2.5, and Pb1.0Se5.0, respectively. The coleus plants were kept in full-strength MHNS without Pb and Se as the control treatment (denoted Pb0Se0). The solution was renewed every 7 days and was aerated continuously during the acclimatization period, and pH was maintained at 6.0-6.5. After the addition of Pb and the different concentrations of Se to the nutrient medium, the loss of water via transpiration was replenished by frequent additions of deionized water to

maintain a constant volume. Plants were kept in a growth chamber with an 8 h light period at a light intensity of 450 μmol/m²/s, 25ºC/20ºC (day/night) temperature and 60-70% relative humidity. Plants were harvested 21 days after each treatment. Upon harvest, each plant was separated into roots, stems, and leaves, and killed out for 30 min at 105ºC in an air blowing thermostatic oven, then dried to constant weight at 65ºC for FTIR.

Measure Method

For FTIR analysis, the roots of coleus plants were oven-dried for 12 h at 65ºC and ground to a fine powder with an agate mortar, followed by sieving through a 150 μm mesh. Roots (1.0 mg) were then mixed with 100 mg KBr and pressed into pellets. Each pellet was immediately placed into a sample holder and FTIR spectra (FTIR Nicolet 5700, Thermo Nicolet Corporation, Wisconsin, USA) were recorded with a resolution of 4 cm⁻¹ and 64 scans in the range of 4,000-400 cm⁻¹. Each root made 9 ingot pieces that collected spectra, and the average was taken as the roots spectra.

Statistical Analysis

OMNIC E.S.P.5.1 intelligent software and ATR correction were used for determining the background value before each treatment sample was measured. The spectra of FTIR was taken under Pb stress with different concentrations of Se treatments, and then the characteristic peak was screened according to the peak absorbance values. Treatments were analyzed using SigmaPlot12.0 (SYSTAT Software Inc., California, USA), 2D Shige software created by Shigeaki Morita (Kwansei-Gakuin University, Japan), and OriginPro Version 8.5 (OriginLab Corporation, Northampton, USA) for 1D and 2D correlation analysis of FTIR spectra.

Results and Discussion

1D-FTIR Spectra Changes Analysis

FTIR is useful for analyzing organic chemical composition as it can identify different functional groups that produce bond absorptions at different locations and intensities on the FTIR spectrum. Recognizing where the absorptions generated by the main functional groups occur can identify the properties, the formation, and the changes of chemical composition containing functional groups under different treatment conditions. The roots were characterized by FTIR spectroscopy to investigate the chemical differences between coleus roots under Pb-induced stress and in the presence of different concentrations of Se. Table 1 shows the important spectral bands and the stretching vibration of their corresponding functional group assignments according to the literature. The Bands at 628-915 cm⁻¹ were assigned to be aromatic C-H out-of-plane bending. The bands at 1,000-1,033 cm⁻¹ were attributed to C-O stretching of polysaccharides. Absorption bands were noted at 1,270 cm⁻¹ (C-O stretching of polysaccharides), 1,300-1,333 cm⁻¹ (CH_2 bending of structural carbohydrates), 1,384 cm⁻¹ (CH_3 bending of lipids/proteins), 1,416 cm⁻¹ (CH_2 stretching of polysaccharide), 1,645 cm⁻¹ (aromatic C=C stretching), 2,130-2,353 cm⁻¹ (C=O stretching of CO_2), 2,850-2,922 cm⁻¹ (asymmetrical CH_2 and symmetrical CH_2 stretching of lipid/carbohydrate), and 3,410-3,900 cm⁻¹ (O-H stretching of water and N-H stretching of protein amide A).

The FTIR spectra of *Coleus blumei* roots exposed to Pb stress with different concentrations of Se treatments are presented in Fig. 1. The peak shape remained basically unchanged among the roots under Pb-induced stress and different concentrations of Se. However, the peak strength did change and there was noticeable displacement of some peaks, as well as emergence/disappearance of some peaks (Fig. 1 and Table 2). This indicates that there were

Table 1. Functional groups assignment of FTIR bands.

| Wave number (cm⁻¹)	Vibrating type *of functional groups*
3,410-3,900	O-H stretching of Water [33-35]; N-H stretching of protein amide A [32]
2,850-2,922	Asymmetrical CH_2 and Symmetrical CH_2 stretching of lipid/carbohydrate [32]
2,130-2,353	C=O stretching of CO_2 [30-31]
1,645	Aromatic C=C stretching [29]
1,416	CH_2 stretching of polysaccharide [28]
1,384	CH_3 bending of lipids/proteins [24]
1,300-1,333	CH_2 bending of structural carbohydrates [26-27]
1,270	C-O stretching of polysaccharides [25]
1,000-1,033	C-O stretching of polysaccharides [24]
628-915	Aromatic C–H out-of-plane bending [20-23]
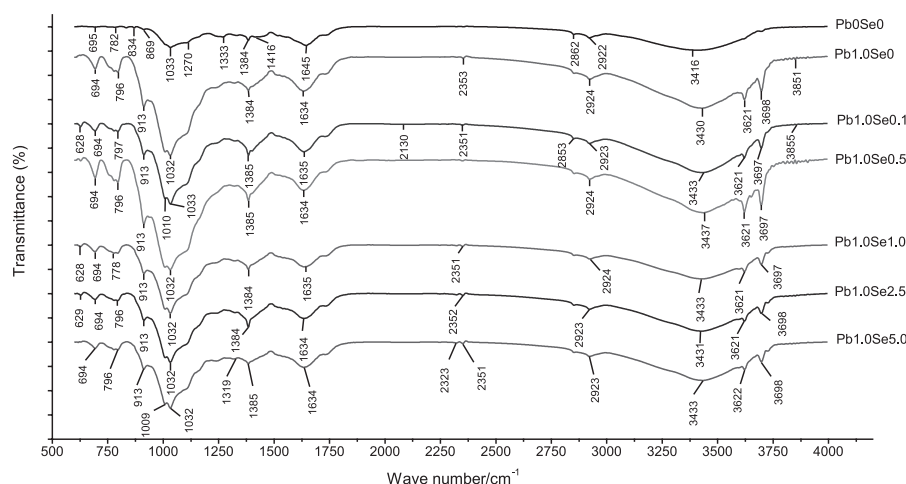
Fig. 1. FTIR spectra of *Coleus blumei* roots under Pb stress with different concentration of Se treatments – Pb0Se0: Pb 0 mmol/L + Se 0 mmol/L; Pb1.0Se0: Pb 1.0 mmol/L + Se 0 mmol/L; Pb1.0Se0.1: Pb 1.0 mmol/L + Se 0.1 mmol/L; Pb1.0Se0.5: Pb 1.0 mmol/L + Se 0.5 mmol/L; Pb1.0Se1.0: Pb 1.0 mmol/L + Se 1.0 mmol/L; Pb1.0Se2.5: Pb 1.0 mmol/L + Se 2.5 mmol/L; Pb1.0Se5.0: Pb 1.0 mmol/L + Se 5.0 mmol/L; the same below.

no changes in the chemical composition of the roots, but that their contents were influenced by treatment with Pb and Se. This finding is consistent with results from recent reports on grape pomace [36] and meager [37]. The absorption peaks displacement of certain functional groups involved in heavy metal adsorption changes to different degrees, e.g., the absorption peak of OH group (3,416-3,900 cm^{-1}), and carbonyl group (1,000-1,100 cm^{-1}, and 1,270 cm^{-1}), which may act as Pb ligands and participate in the processes of Pb sequestration in coleus roots with exogenous Se treatments [38]. In addition, a new peak appeared at 2,130-2,353 cm^{-1} (C=O stretching of CO_2) under Pb stress with different concentration of Se treatments, except for Pb1.0Se0.5, which demonstrates the existence of transition-metal complexes affecting intercellular CO_2 [39].

Semi-quantitative data are used to compare spectral data from samples in order to obtain information on how different functional groups respond differently to environmental changes [40-41]. The following semi-quantitative measurements of FTIR spectra were analyzed by integrating the total peak area from: (1) 3,410-3,900 cm^{-1} (OH, aliphatic O–H stretching); (2) 1,645 cm^{-1} (C1, aromatic carbon groups C=C); (3) 1,420-1,300 cm^{-1} (CH, CH_2 and CH_3 compounds); (4) 1,000-1,270 cm^{-1} (Ox1, contribution of C-O groups); and (6) 915-628 cm^{-1} (Ar, aromatic C–H out-of-plane bending).

The CH_2/CH_3 ratio is the sum of the CH_2 peak areas (1,416 and 2,850-2,922 cm^{-1}) divided by the sum of the CH_3 peak areas (1,384 cm^{-1}), which relates to aliphatic chain length and degree of branching of aliphatic side groups. A higher value implies comparatively longer and straighter chains; a lower value, shorter and more branched chains.

The OH/Ox1 ratio is the ratio of the integrated area of the O-H stretching region (3,410-3,900 cm^{-1}) divided by the integrated area of the oxygenated group region (1,000-1,270 cm^{-1}). This is the relative contribution of O-H stretching to the combined contribution of oxygen-containing groups, and can be inferred oxygen-containing groups decreasing from higher values.

The Ox1/C1 ratio is the ratio of the integrated area of the (C-O) stretching region (1,000-1,270 cm^{-1} and the integrated area of the aromatic carbon (C=C) groups (1,645 cm^{-1}). This is the relative contribution of C-O to aromatic carbon groups, and higher values indicate increasing ratios of C-O groups to aromatic carbon groups.

Ar/CHx is the ratio of the integrated area of the aromatic C–H out-of-plane bending (915-628 cm^{-1}) and the integrated area of the CH_2 and CH_3 stretching region (2,850-2,922 and 1,420-1,300 cm^{-1}). This is the contribution of aromatic C–H out-of-plane bending modes to aliphatic C–H stretching bands, and higher values indicate higher aromaticity in the organic matter.

The A factor is defined by the integrated area of the aliphatic stretching region (2,850-2,922 cm^{-1}) divided by the sum of the integrated areas of the aliphatic stretching region (2,850-2,922 cm^{-1}) and aromatic carbon structures (1,645 cm^{-1}), representing changes in the relative intensities of the aliphatic groups.

The C factor is defined by the integrated area of the oxygenated group region (1,000-1,270 cm^{-1}) divided by the sum of the integrated areas of the oxygenated group region (1,000-1,270 cm^{-1}) and aromatic carbon structures (1,645 cm^{-1}), representing changes in the C-O groups.

All these ratios could also be used for comparative purposes, providing valuable information on the changes of chemical functional groups in *C. blumei* roots under Pb stress with different concentrations of Se treatments in an attempt to identify the differences in functional groups according to the proposal of Ganz and Kalkreuth [42].

Changes in the FTIR bands were used to obtain semi-quantitative data for Pb stress with different

Table 2. FTIR typical peak of Coleus blumei roots under lead stress with different concentrations of Se treatment.

Treatments	Peak positions (cm⁻¹)																					Peak number
	628	695	782	834	869	913	1010	1033	1270	1333	1384	1416	1645	2130	2353	2862	2922	3416	3621	3698	3851	
PbOSe0		695	782	834	869			1033	1270	1333	1384	1416	1645			2862	2922	3416				13
Pb1.0Se0		694	796			913		1032			1384		1634		2353		2924	3430	3621	3698	3851	12
Pb1.0Se0.1	628	694	797			913	1010	1033			1385		1635	2130	2351	2853	2923	3433	3621	3697	3855	16
Pb1.0Se0.5		694	796			913		1032			1385		1634				2924	3437	3621	3697		10
Pb1.0Se1.0	628	694	778			913		1032			1384		1635		2351		2924	3433	3621	3697		12
Pb1.0Se2.5	629	694	796			913		1032			1384		1634		2352		2923	3431	3621	3698		12
Pb1.0Se5.0		694	796			913	1009	1032		1319	1385		1634	2323	2351		2923	3433	3622	3698		14

concentrations of Se treatments (Table 3). The CH_2/CH_3 ratio can be used as a discriminatory function for chemical composition [43]. The CH_2/CH_3 ratio in *C. blumei* roots for Pb1.0Se0 showed the lowest value (0.66) in this study (Table 3). This indicates that *C. blumei* roots under Pb stress without Se had longer and straighter aliphatic chains compared with PbOSe0. However, the CH_2/CH_3 ratio of *C. blumei* roots under Pb stress with different concentrations of Se treatments showed lower values, except for the Pb1.0Se0.1 treatment. This indicates that the length and straightness of the aliphatic chains in the *C. blumei* roots were increased under Pb stress with Pb1.0Se0.5, Pb1.0Se1.0, Pb1.0Se2.5, and Pb1.0Se5.0 – especially the Pb1.0Se0.5 treatment. The Pb1.0Se0.1 treatment had a higher value (4.16), indicating that the *C. blumei* roots had shorter and more branched aliphatic chains under Pb stress with 0.1 mM Se treatment.

For the OH/Ox1 ratio, the values for the Pb1.0Se0 treatment decreased significantly compared with the PbOSe0 treatment, which indicates a larger contribution of oxygen-containing groups. However, the OH/Ox1ratio under Pb stress with different concentrations of Se treatments shows lower and similar values except for the Pb1.0Se2.5 treatment. The lowest value was for the Pb1.0Se0.5 treatment, which indicates the largest contribution of oxygen-containing groups. In addition, the highest value was for the Pb1.0Se2.5 treatment, which indicates an increase in OH contribution.

For the Ox1/C1 ratio, Pb1.0Se0 treatment showed higher values compared with the PbOSe0 treatment, which indicates increasing ratios of C-O groups to aromatic carbon groups. However, the OH/Ox1ratio under Pb stress with different concentrations of Se treatments decreased, except for the Pb1.0Se0.1 and Pb1.0Se0.5 treatments, which indicates a higher oxidation of organic matter in the Pb1.0Se1.0, Pb1.0Se2.5, and Pb1.0Se5.0 treatments. Meanwhile, there were higher values for the Pb1.0Se0.1 and Pb1.0Se0.5 treatments compared with other treatment concentrations of Se, which indicates increasing ratios of C-O groups to aromatic carbon groups.

With respect to the aromatic Ar/CHx ratio, the Pb1.0Se0 treatment shows higher values compared to the PbOSe0 treatment, which indicates a higher aromaticity in the organic matter under Pb stress. However, the Ar/CHx ratio under Pb stress with different concentrations of Se treatments decreased, except for the Pb1.0Se0.5 treatment, which showed that the aromaticity of the organic matter was decreasing, especially for the Pb1.0Se0.1 treatment. However, the Pb1.0Se0.5 treatment showed the highest value, which indicates higher aromaticity in the organic matter.

Finally, the compressions of *C. blumei* roots for the Pb1.0Se0 treatment were characterized by low values for A factor and high values for C factor, compared with the PbOSe0, which indicates low contents of aliphatic, and high contents of oxygen-containing compounds (Table 3). The compressions of *C. blumei* roots for Pb stress with the 0.1 mM Se treatment were characterized by high values

Table 3. Comparison of semi-quantitative FTIR data of Coleus blumei roots under lead stress with different concentrations of Se treatments.

Treatments	Ratio					
	CH_2/CH_3	OH/Ox1	Ox1/C1	Ar/CHx	A factor	C factor
Pb0Se0	5.04	4.08	1.06	0.03	0.49	0.55
Pb1.0Se0	0.66	1.52	3.90	0.48	0.35	0.79
Pb1.0Se0.1	4.16	1.41	5.24	0.24	0.62	0.84
Pb1.0Se0.5	0.49	0.98	4.86	0.68	0.27	0.83
Pb1.0Se1.0	0.65	1.54	3.69	0.42	0.35	0.79
Pb1.0Se2.5	0.54	1.79	3.27	0.31	0.35	0.77
Pb1.0Se5.0	0.53	1.39	3.84	0.34	0.32	0.79

for A factor and high values for C factor, compared with other concentration of Se treatments, which indicates high contents of aliphatic and high contents of oxygen-containing compounds, respectively.

2D-FTIR Correlation Spectra Analysis

The synchronous and asynchronous 2D-FTIR correlation spectra of *C. blumei* roots under Pb stress with different concentrations of Se treatments in the region of 929-1,800 cm^{-1} are shown in Figs 2-8.

Fig. 2a shows the synchronous 2D correlation spectrum of Pb0Se0 treatment based on autocorrelation calculations in the region of 1,000-1,645 cm^{-1}. The peak at 1,000-1,033 cm^{-1} was attributed to the C-O stretching of polysaccharides in *C. blumei* roots. The two peaks observed at 1,270 cm^{-1} and 1,384 cm^{-1} were attributed to the C-O stretching of polysaccharides and CH$_3$ bending of lipids/proteins in *C. blumei* roots, respectively. The peak at 1,645 cm^{-1} was assigned to the aromatic C=C stretching vibration in *C. blumei* roots. Two positive cross-peaks observed at (1,033, 1,645) cm^{-1} and (1,270, 1,384) cm^{-1}, and the 5 negative cross peak observed at (1,033, 1,270)

cm^{-1}, (1,033, 1,384) cm^{-1}, (1,645, 1,270) cm^{-1}, (1,645, 1,384) cm^{-1}, and (1,384, 1,270) cm^{-1} result from the orientation of C-O, aromatic C=C, and CH$_3$ vibrations generated at the same time. According to 2D correlation rules [44], the functional groups of C-O, aromatic C=C, and CH$_3$ had a cooperative effect, but had the reverse direction of the intensity variations in these 2 correlated stretching vibration modes. In the asynchronous spectrum of the Pb0Se0 treatment (Fig. 2b), according to the rule of Noda [44], the negative sign of the cross-peaks at (1,033, 1,270) cm^{-1}, (1,033, 1,384) cm^{-1}, (1,645, 1,270) cm^{-1}, (1,645, 1,384) cm^{-1}, and (1,384, 1,270) cm^{-1} indicates that the intensity change of the symmetric stretching vibration of functional groups occurs prior to that of the asymmetric one. On the basis of Noda's rule [44-45] and the method of Murayama et al. [46], the following sequence of the intensity variations was deduced: C-O stretching of polysaccharides (1,270 cm^{-1}) $\approx$ CH$_2$ and CH$_3$ in lipids (1,384 cm^{-1})>C-O stretching of polysaccharides (1,033 cm^{-1}) $\approx$ aromatic C=C stretching (1,654 cm^{-1}).

In the synchronous 2D correlation spectrum of the Pb1.0Se0 treatment (Fig. 3a), one auto-peak at
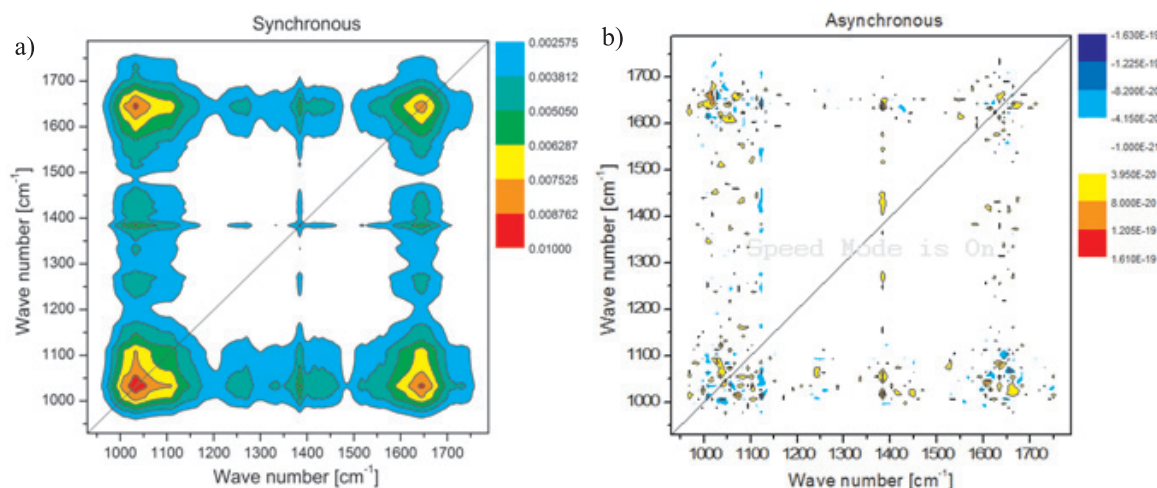
Fig. 2. Synchronous and asynchronous 2D-FTIR correlation spectra of *Coleus blumei* roots without lead and selenium.
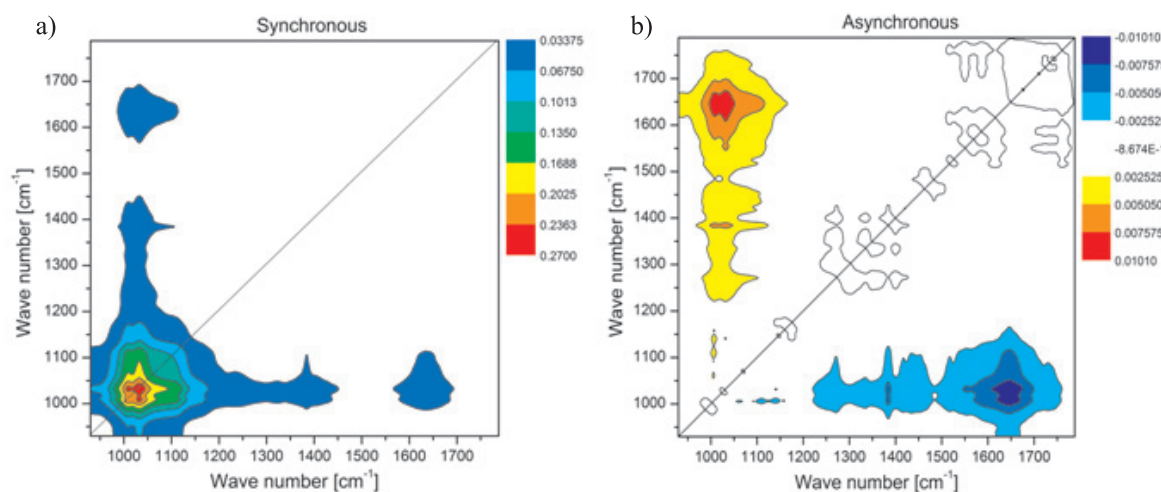
Fig. 3. Synchronous and asynchronous 2D-FTIR correlation spectra of *Coleus blumei* roots under 0 mM and 1.0 mM lead treatments.

$\Phi(1{,}000\text{-}1{,}150, 1{,}000\text{-}1{,}150) > 0$, one positive cross-peak at $\Phi(1{,}384, 1{,}645) > 0$, and 2 negative cross-peaks at $\Phi(1{,}000\text{-}1{,}150, 1{,}384) < 0$ and $\Phi(1{,}000\text{-}1{,}150, 1{,}645) < 0$ were observed. This implies that the band from $1{,}000\text{-}1{,}150$ cm^{-1} varies in the opposite direction to the bands at 1,384 and 1,645 cm^{-1}. As has already been mentioned, these bands were assigned to C-O stretching vibration in polysaccharides, CH$_3$ bending of lipids/proteins, and aromatic C=C stretching vibration, respectively. Thus it was observed that the C-O stretching vibrations (1,000-1,150 cm^{-1}) vary in the opposite direction to the CH$_3$ stretching (1,384 cm^{-1}) and aromatic C=C stretching (1,645 cm^{-1}) under Pb treatment, compared with the Pb0Se0 treatment. Three bands at 1,125 cm^{-1}, 1,384 cm^{-1}, and 1,645 cm^{-1} were identified in the asynchronous 2D correlation spectrum of the Pb1.0Se0 treatment (Fig. 3b). The sequence of the spectral intensity changes was obtained as follows: 1,125 cm^{-1} > 1,384 cm^{-1} > 1,645 cm^{-1}. This sequence means that the moment of C-O groups (1,125 cm^{-1}) in

polysaccharides changes first, followed by the CH$_3$ stretching vibration in lipids/proteins, and the C=C stretching of the aromatic skeleton under Pb stress.

In the synchronous 2D correlation spectrum of the Pb1.0Se0.1 treatment (Fig. 4a), one auto-peak at $\Phi(1{,}000\text{-}1{,}150, 1{,}000\text{-}1{,}150) > 0$, one positive cross-peak at $\Phi(1{,}384, 1{,}645) > 0$, and 3 negative cross-peaks at $\Phi(1{,}000\text{-}1{,}150, 1{,}270) < 0$, $\Phi(1{,}000\text{-}1{,}150, 1{,}333) < 0$ and $\Phi(1{,}000\text{-}1{,}150, 1{,}645) < 0$ were observed. This implies that the band from 1,000-1,150 cm^{-1} varies in the opposite direction to the bands at 1,384 and 1,645 cm^{-1}. This indicates that the C-O stretching vibrations (1,000-1,150 cm^{-1}) vary in the opposite direction to the C-O stretching (1,270 cm^{-1}), the CH$_3$ stretching (1,384 cm^{-1}), and the aromatic C=C stretching (1,645 cm^{-1}) under the Pb1.0Se0.1 treatment, compared with the Pb1.0Se0 treatment. Four bands at 1,033 cm^{-1}, 1,270 cm^{-1}, 1,333 cm^{-1}, and 1,645 cm^{-1} were identified in the asynchronous 2D correlation spectrum of the Pb1.0Se0.1 treatment (Fig. 4b). The sequence of the spectral intensity changes was obtained as follows:
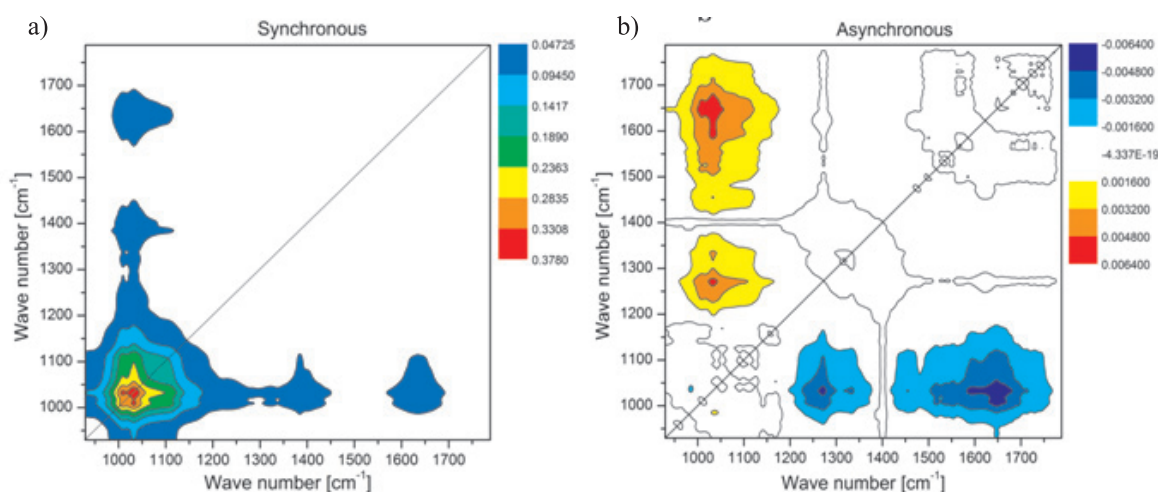

Fig. 4. Synchronous and asynchronous 2D-FTIR correlation spectra of *Coleus blumei* roots under 0 mM and 1.0 mM lead with 0.1 mM Se treatment.
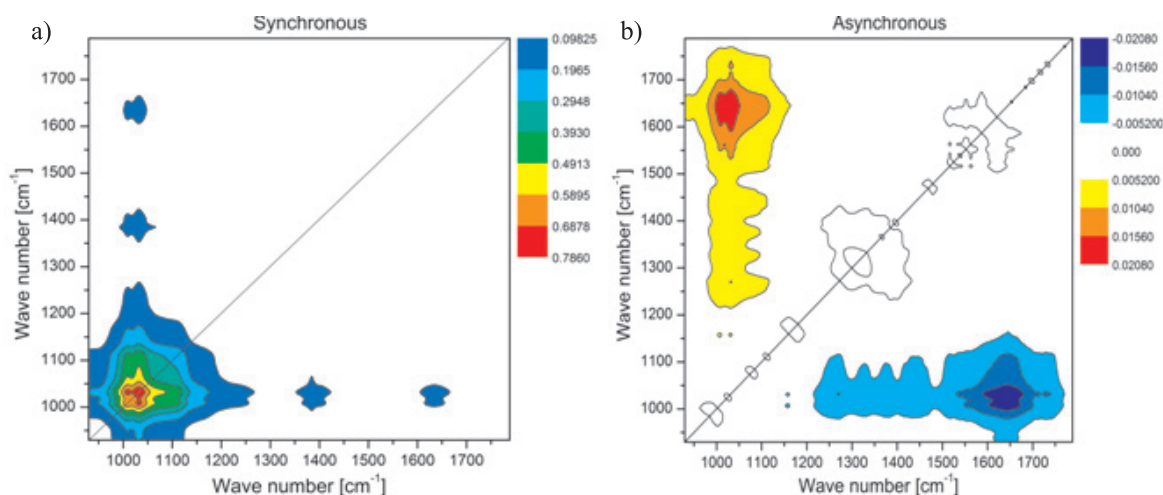
Fig. 5. Synchronous and asynchronous 2D-FTIR correlation spectra of *Coleus blumei* roots under 0 mM and 1.0 mM lead with 0.5 mM Se treatment.

1,033 cm^{-1} > 1,270 cm^{-1} >1,333 cm^{-1} > 1,645 cm^{-1}. This sequence means that the moment of the C-O groups (1,033 cm^{-1}) in polysaccharides changes first, followed by the C-O groups (1,270 cm^{-1}), CH$_2$ stretching vibration in lipids/proteins (1,333 cm^{-1}), and the C=C stretching of the aromatic skeleton (1,645 cm^{-1}) under Pb stress with 0.1mM Se.

In the synchronous 2D correlation spectrum of the Pb1.0Se0.5 treatment (Fig. 5a), one auto-peak at Φ(1,000-1,150, 1,000-1,150) > 0, one positive cross-peak at Φ(1,384, 1,645) > 0, and 2 negative cross-peaks at Φ(1,000-1,150, 1,384) < 0 and Φ(1,000-1,150, 1,645) < 0 were observed. This implies that the band at 1,000-1,150 cm^{-1} varies in the opposite direction to the bands at 1,384 cm^{-1} and 1,645 cm^{-1}. This means that the C-O stretching vibrations (1,000-1,150 cm^{-1}) vary in the opposite direction to the CH$_3$ stretching (1,384 cm^{-1}) and aromatic C=C stretching (1,645 cm^{-1}) under the Pb1.0Se0.5 treatment,

compared with the Pb1.0Se0 treatment. Three bands at 1,125 cm^{-1}, 1,270 cm^{-1}, and 1,645 cm^{-1} were identified in the asynchronous 2D correlation spectrum of the Pb1.0Se0.5 treatment (Fig. 5b). The sequence of the spectral intensity changes was obtained as follows: 1,125 cm^{-1} > 1,270 cm^{-1} > 1,645 cm^{-1}. This sequence means that the moment of the C-O groups in polysaccharides changes first, followed by the C=C stretching of the aromatic skeleton under Pb stress with 0.5 mM Se.

In the synchronous 2D correlation spectrum of the Pb1.0Se1.0 treatment (Fig. 6a), one auto-peak at Φ(1,000-1,150, 1,000-1,150) > 0, one positive cross-peak at Φ(1,384, 1,645) > 0, and two negative cross-peaks at Φ(1,000-1,150, 1,384) < 0 and Φ(1,000-1,150, 1,645) < 0 were observed. This implies that the band at 1,000-1,150 cm^{-1} varies in the opposite direction to the bands at 1,384 cm^{-1} and 1,645 cm^{-1},
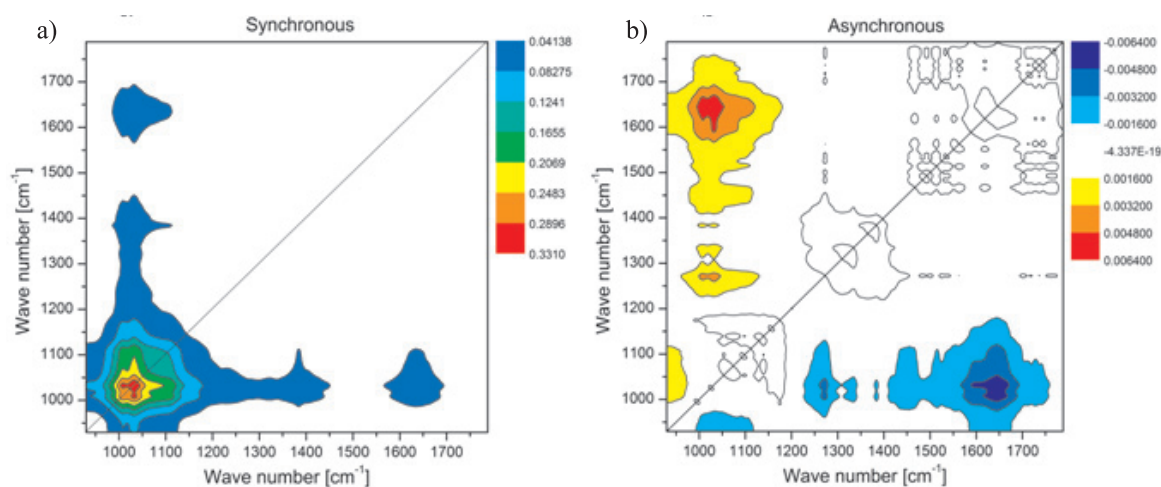

Fig. 6. Synchronous and asynchronous 2D-FTIR correlation spectra of *Coleus blumei* roots under 0 mM and 1.0 mM lead with 1.0 mM Se treatment.
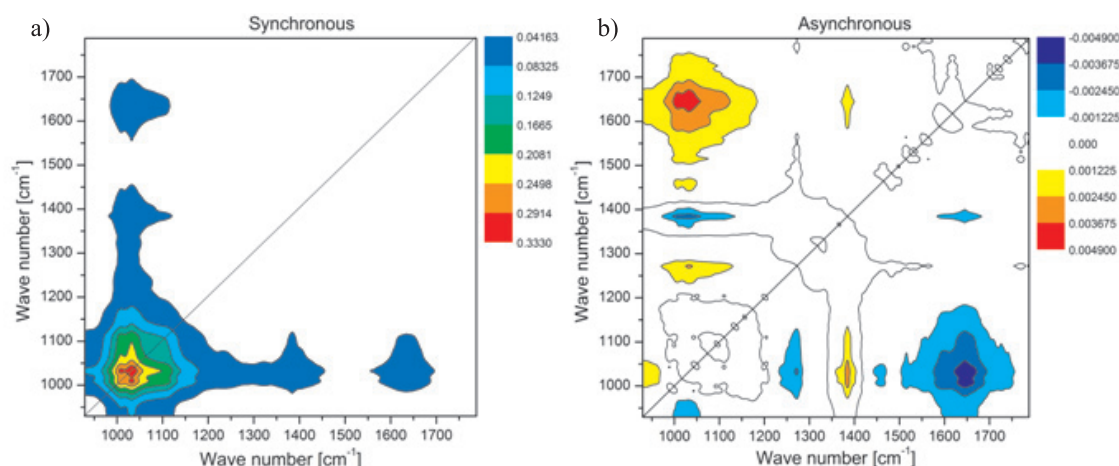
Fig. 7. Synchronous and asynchronous 2D-FTIR correlation spectra of *Coleus blumei* roots under 0 mM and 1.0 mM lead with 2.5 mM Se treatment.

which means that the C-O stretching vibrations (1,000-1,150 cm^{-1}) vary in the opposite direction to the CH$_3$ stretching (1,384 cm^{-1}) and aromatic C=C stretching (1,645 cm^{-1}) under the Pb1.0Se1.0 treatment compared with the Pb1.0Se0 treatment. Four bands at 1,033 cm^{-1}, 1,270 cm^{-1}, 1,384 cm^{-1}, and 1,645 cm^{-1} were identified in the asynchronous 2D correlation spectrum of the Pb1.0Se1.0 treatment (Fig. 6b). The sequence of the spectral intensity changes was obtained as follows: 1,033 cm^{-1} > 1,384 cm^{-1} > 1,270 cm^{-1} > 1,645 cm^{-1}. This sequence means that the moment of the C-O groups in polysaccharides changes first, followed by the CH$_3$ stretching vibration in the lipids/proteins, the C-O stretching of the polysaccharides, and the C=C stretching of the aromatic skeleton under Pb stress with 1.0 mM Se.

In the synchronous 2D correlation spectrum of the Pb1.0Se2.5 treatment (Fig. 7a), one auto-peak at Φ(1,000-1,150, 1,000-1,150) > 0, one positive cross-peak at Φ(1,384, 1,645) > 0, and 2 negative cross-peaks

at Φ(1,000-1,150, 1,384) < 0 and Φ(1,000-1,150, 1,645) < 0 were observed. This implies that the band at 1,000-1,150 cm^{-1} varies in the opposite direction to the bands at 1,384 cm^{-1} and 1,645 cm^{-1}, which means that the C-O stretching vibrations (1,000-1,150 cm^{-1}) vary in the opposite direction to the CH$_3$ stretching (1,384 cm^{-1}) and the aromatic C=C stretching (1,645 cm^{-1}) under the Pb1.0Se2.5 treatment compared with the Pb1.0Se0 treatment. Five bands at 1,033 cm^{-1}, 1,270 cm^{-1}, 1,384 cm^{-1}, 1,416 cm^{-1}, and 1,645 cm^{-1} were identified in the asynchronous 2D correlation spectrum of the Pb1.0Se2.5 treatment (Fig. 7b). The sequence of the spectral intensity changes was obtained as follows: 1,033 cm^{-1} > 1,416 cm^{-1} > 1,270 cm^{-1} > 1,384 cm^{-1} > 1,645 cm^{-1}. This sequence means that the moment of the C-O (1,033 cm^{-1}) groups in the polysaccharides change first, followed by the CH$_2$ groups (1,416 cm^{-1}) and the C-O stretching (1,270 cm^{-1}) of the polysaccharides, the CH$_3$ stretching vibration in the lipids/proteins (1,384 cm^{-1}), and the C=C stretching
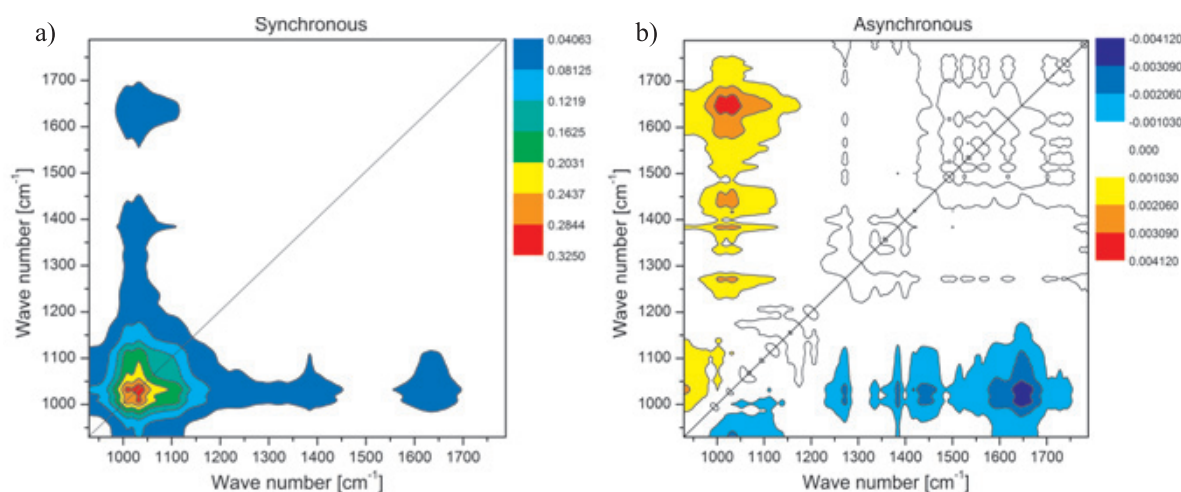

Fig. 8. Synchronous and asynchronous 2D-FTIR correlation spectra of *Coleus blumei* roots under 0 mM and 1.0 mM lead with 5.0 mM Se treatment.

of the aromatic skeleton (1,645 cm^{-1}) under Pb stress with 2.5 mM Se.

In the synchronous 2D correlation spectrum of the Pb1.0Se5.0 treatment (Fig. 8a), one auto-peak at $\Phi(1,000-1,150, 1,000-1,150) > 0$, one positive cross-peak at $\Phi(1,384, 1,645) > 0$, and 2 negative cross-peaks at $\Phi(1,000-1,150, 1,384) < 0$ and $\Phi(1,000-1,150, 1,645) < 0$ were observed. This implies that the band at 1,000-1,150 cm^{-1} varies in the opposite direction to the bands at 1,384 cm^{-1} and 1,645 cm^{-1}. This means that the C-O stretching vibrations (1,000-1,150 cm^{-1}) vary in the opposite direction to the CH$_3$ stretching (1,384 cm^{-1}) and the aromatic C=C stretching (1,645 cm^{-1}) under the Pb1.0Se5.0 treatment, compared to the Pb1.0Se0 treatment. Five bands at 1,033 cm^{-1}, 1,270 cm^{-1}, 1,384 cm^{-1}, 1,416 cm^{-1}, and 1,645 cm^{-1} were identified in the asynchronous 2D correlation spectrum of the Pb1.0Se5.0 treatment (Fig. 8b). The sequence of the spectral intensity changes was obtained as follows: 1,033 cm^{-1}, 1,270 cm^{-1} > 1,416 cm^{-1} > 1,384 cm^{-1} > 1,645 cm^{-1}. This sequence means that the moment of the C-O groups in the polysaccharides changes first, followed by the CH$_2$ groups in the polysaccharides, the CH$_3$ stretching vibration in the lipids/proteins, and the C=C stretching of the aromatic skeleton under Pb stress with 5.0 mM Se.

Based on the 2D-FTIR correlation spectra data, we found that most sensitive to Pb stress were the C-O groups from the polysaccharides, followed by the CH$_3$ group in the lipids/proteins, and the C=C group of the aromatic skeleton. This indicates that the carboxyl (C=O) and aliphatic chains are mainly responsible for lead adsorption in *C. blumei* roots. Other studies have also reported that carboxyl (C=O) and phenol (OH) groups make important contributions to Pb^{2+} sorption [47, 48]. However, with the addition of different concentrations of Se during Pb stress, these functional groups were responsible for Pb adsorption, as changes in the peaks were observed around the wavelengths of these groups. The Se concentration-dependent changes appeared in the infrared regions characteristic of the C=O, CH$_2$, CH$_3$, and C=C stretching frequencies of the polysaccharides and the lipids/proteins. These results were in accordance with semi-quantitative data from the above 1D-FTIR spectra.

Conclusions

The peak shapes remained basically unchanged in *C. blumei* roots exposed to Pb stress with different concentrations of Se treatments, and the wave number of the absorption peaks remained stationary, which indicates that the chemical composition in the roots had not changed. However, there is a significant difference in the absorption peak strength, which is influenced by the chemical composition. Semi-quantitative data indicate that there were obvious differences among the characteristics of the organic functional groups.

The FTIR spectrum confirms the presence of various functional groups from the responses to abiotic stresses in the plant, which may influence the reduction process and stabilization of heavy metals.

There were obvious differences among the 2D-FTIR correlation spectra of *C. blumei* roots in the region of 929-1,800 cm^{-1} under Pb stress with different concentrations of Se treatments. Significant differences between the 2D-FTIR correlation spectra of *C. blumei* roots are likely to be related to differences in chemical composition and its structure. The high resolution 2D-FTIR technology based on similar samples as the one-dimensional infrared spectrum can provide the microscopic information from the dynamic changes of chemical composition structure resulting from Se concentration changes. The results demonstrate that 2D-FTIR correlation spectroscopy may be a convenient and effective method in the study of plant molecular interactions under environmental stress.

References

1. FARD K.G., GHASEMNEZHAD M., ZAKIZADEH H., KAFI M., REJALI F. Evaluation of six cold-season turfgrasses responses to lead phytotoxicity for screening tolerant species. Caspian J. Environ. Sci. **14** (3), 215, **2016**.
2. THUPPIL V., TANNIR S. Treating lead toxicity: Possibilities beyond synthetic chelation. Journal of Krishna Institute of Medical Sciences University (JKIMSU), **2**(1), 4, **2013**.
3. SHARMA P., DUBEY R.S. Lead toxicity in plants, Braz. J. Plant Physiol. **17** (1), 35, **2005**.
4. BAGHAIE A., KHOSHGOFTARMANESH A., AFYUNI M. Phytoavailability of lead (Pb) for corn and sunflower as affected by Pb-enriched sewage sludge and cow manure. J. Residuals Sci. Tech. **13**(4), 251, **2016**.
5. JORDAO C.P., NASCENTES C.C., CECON P.R., FONTES R.L.F., PEREIRA J.L. Heavy metal availability in soil amended with composted urban solid wastes. Environ. Monit. Assess. **112** (1-3), 309, **2016**.
6. LIU D., JJIANG W., LIU C., XIN C., HOU W. Uptake and accumulation of lead by roots, hypocotyls and shoots of Indian mustard Brassica juncea L.. Bioresource Technol. **71** (3), 273, **2000**.

7. MROCZEK-ZDYRSKA M., WÓJCIK M. The influence of selenium on root growth and oxidative stress induced by lead in *Vicia faba* L. minor plants. Biol. Trace Elem. Res. **147** (1-3), 320, **2012**.

8. MROCZEK-ZDYRSKA M., STRUBIŃSKA J., HANAKA A. Selenium improves physiological parameters and alleviates oxidative stress in shoots of lead-exposed *Vicia faba* L. *minor* plants grown under phosphorus-deficient conditions. J. Plant Growth Regul. **36** (1), 186, **2016**.

9. ELGAML S.A., KHALIL R., HASHISH E.A., EL-MUR A. Protective effects of selenium and alpha-tocopherol against lead induced hepatic and renal toxicity in Oreochromis niloticus. J. Aquac. Res. Development. **6** (1), 1, **2015**.

10. HU Y., NORTON G.J., DUAN G., HUANG Y.C., LIU Y.X. Effect of selenium fertilization on the accumulation of cadmium and lead in rice plants. Plant and Soil. **384** (1), 131, **2014**.

11. HE P.P., LV X.Z., WANG G.Y. Effects of Se and Zn supplementation on the antagonism against Pb and Cd in vegetables. Environ. Int. **30** (2), 167, **2004**.

12. POPESCU M.C., ZANOAGA M., MAMUNYA Y., MYSHAK V., VASILE C. Two dimensional infrared correlation spectroscopy studies of wood-plastic composites with a copolyamide as matrix. J. Optoelectron Adv. M. **9** (4), 923, **2007**.

13. LIU X.Y., ZHOU T., WANG X.C., ZHANG J.H. Investigation of selective molecular interactions using two-dimensional Fourier transform IR spectroscopy. Anal. Bioanal. Chem. **397** (1), 339, **2010**.

14. PARROTTA L., GURRRIERO G., SERGEANT K., CAI G., HAUSMAN J.F. Target or barrier? The cell wall of early- and later-diverging plants vs cadmium toxicity: differences in the response mechanisms. Front Plant Sci. **6** (133), 1, **2015**.

15. UCHIMIYA M., BANNON D.I., WARTELLE L.H. Retention of heavy metals by carboxyl functional groups of biochars in small arms range soil. J. Agric. Food Chem. **60** (7), 1798, **2012**.

16. KHABIBI J., SYAFII W., SARI R.K. Reducing hazardous heavy metal ions using mangium bark waste. Environ. Sci. Pollut. Res. **23** (6), 1, **2016**.

17. YUAN J.H., HU, M.H., ZHOU Z.H. Selenium alleviates coleus from oxidative damage under Pb stress by resource allocation and antioxidant defense system. Res. J. Appl. Sci. Eng. Technol. **6** (9), 1606, **2013**.

18. HOAGLAND D.R., ARMON D.I. The water culture method for growing plants without soil, Cal. Agri. Expt. Sta. Cir. **347** (5406), 357, **1950**.

19. ZHAO L.Z., MAO D., LIN Z.Y. Effects of different nutrient solution on pigment content and photosynthesis of *Coleus blumei*. Chinese Guangdong Agricultural Sciences, (6), 30, **2007** [In Chinese].

20. WANG Y.L., LI Y.N., SUN W.W., SONG Q. Research on chemical substance in pueraria lobata by FTIR and HPLC. Modernization of Traditional Chinese Medicine and Materia Medica-World Science and Technology. **16** (2), 379, **2014**.

21. KUBBA R.M., SAMAWI K.A. Studying of frequencies, normal modes of vibration and electronic charge densities of radialene molecule. Iraqi J. Sci. **54** (4), 753, **2013**.

22. RENGANAYAKIV.,SYAMALA D.,SATHYAMOORTHY R. Growth, Structural and spectral studies on pure and doped ammonium dihydrogen phosphate (ADP) single crystals. Arch. Appl. Sci. Res. **4** (3), 1453, **2012**.

23. BARTOŠOVÁ A.; SOLDÁN M., SIROTIAK M., BLINOVÁ L., MICHALIKOVÁ A. Application of FTIR-ATR spectroscopy for determination of glucose in hydrolysates of selected starches. Res. Papers Faculty Mater. Sci. Technol. Slovak Univ. Technol. **21** (Special Issue), 116, **2013**.

24. HANDS J.R., CLEMENS G., STABLES R., ASHTON K., BRODBET A., DAVIS C., DAWSON T.P., JENKINSON M.D., LEA R.W., WALKER C., BAKER M.J. Brain tumour differentiat ion: rapid stratified serum diagnostics via attenuated total reflection Fourier-transform infrared spectroscopy. J. Neurooncol. **127** (3), 463, **2016**.

25. CAUNII A., PRIBAC G., GROZEA I., GAITIN D., SAMFIRA I. Design of optimal solvent for extraction of bio-active ingredients from six varieties of Medicago sativa. Chem. Cent. J. **6** (1), 123, **2012**.

26. FEO J.C., CASTRO M.A., ROBLES L.C., ALLER A.J. Fourier-transform infrared spectroscopic study of the interactions of selenium species with living bacterial cells. Anal. Bioanal. Chem. **378** (6), 1601, **2004**.

27. YU P.Q. Board-invited review: sensitivity and responses of functional groups to feed processing methods on a molecular basis. J. Anim. Sci. Biotechno. **4** (1), 42, **2012**.

28. MOHANED G.F., SHAHEEN M.S., KHALIL S.K.H., HUSSEIN A.M.S., KAMIL M.M. Application of FTIR spectroscopy for rapid and simultaneous quality determination of some fruit products, Nature & Science, **9** (11), 21, **2011**.

29. RASULI R., MOKARIAN Z., KARIMI R., SHABANZADEH H., ABEDINI Y. Wettability modification of graphene oxide by removal of carboxyl functional groups using non-thermal effects of microwave. Thin Solid Films. **589** (5), 364, **2015**.

30. WAN P., WU J.Y., TAN L.L., ZHANG B.C., YANG K. Research on super-hydrophobic surface of biodegradable magnesium alloys used for vascular stents. Mater. Sci. Eng. C. Mater. Biol. Appl. **33** (5), 2885, **2013**.

31. ZHANG Z.S., TAO Y.J., YANG Z.G., MAI K.C. Preparation and characteristics of nano-$CaCO_3$ supported b-nucleating agent of polypropylene. Eur. Polym. J. **44** (7), 1955, **2008**.

32. DUYGU D.Y., UDOH A.U., OZER T.B., AKBULUT A., ERKAYA I.A., YILDIZ K., GULER D. Fourier transform infrared (FTIR) spectroscopy for identification of Chlorella vulgaris Beijerinck 1890 and Scenedesmus obliquus (Turpin) Kützing 1833. Afr. J. Biotechnol. **11** (16), 3817, **2012**.

33. SZCZEPANIK B., SLOMLIEWICZ P., GARNUSZEK M., CZECH K., DARIUSZ-BANAŚ D., KUBALA-KUKUŚ A., STABRAWA I. The effect of chemical modification on the physico-chemical characteristics of halloysite: FTIR, XRF, and XRD studies. J. Mol. Struct. **1084**, 16, **2015**.

34. XIONG J., ZHU W.S., LI H.M., XU Y.H., JIANG W., XUN S.H., LIU H. Immobilized fenton-like ionic liquid: catalytic performance for oxidative desulfurization. AIChE J. **59** (12), 4696, **2013**.

35. AROKE U.O., EL-NAFATY U.A. XRF, XRD and FTIR properties and characterization of HDTMA-Br surface modified organo-kaolinite clay. Int. J. Emerging Tech. Adv. Eng. **4** (4), 817, **2014**.

36. SOUSA E.C., UCHÔ-THOMAZ A.M.A., CARIOCA J.O.B., MORAIS S.M., LIMA A., MARTINS C.G., ALEXANDRINO C.D., FERREIRAP P.A.T., RODRIGUES A.L.M., RODRIGUES S.P., SILVA J.N., RODRIGUES L.L. Chemical composition and bioactive compounds of grape pomace (*Vitis vinifera* L.), Benitaka variety, grown in the semiarid region of Northeast. Brazil. Food Sci. Technol. **34** (1), 135, **2014**.

37. SIMÕES T., FONSECA S.B., AUGUSTO A., GRANADA L., OZÓRION R.O.A., GONÇALVES J.F.M., PASCOAL L.A.F., SILVA J.H.V., LEMOS M.F.L. Changes in fatty acid profile and chemical composition of meagre (Argyrosomus regius) fed with different lipid and selenium levels. Eur. J. Lipid Sci. Tech. **119** (6), 100, **2017**.

38. SHARMA B., SINGH S., SIDDIQI N.J. Biomedical implications of heavy metals induced imbalances in redox systems. BioMed Res. Int. **2014** (1), 1, **2014**.

39. KHOSHKISH M., BOUHENDI H., VAFAYAN M. Effect of CO_2 fixation reaction on the thermal and dynamic mechanical properties of tetrafunctional epoxy resin. J. Mater. Sci. **49** (19), 6813, **2014**.

40. ZODROW E.L. Molecular self-assembly: hypothesized for "hair" of Macroneuropteris scheuchzeri (Pennsylvanian-age seed-fern). Int. J. Coal Geol. **121**, 14, **2014**.

41. D'ANGELO J.A., ZODROW E.L. Chemometric study of structural groups in medullosalean foliage (Carboniferous, fossil Lagerstätte, Canada): Chemotaxonomic implications. Int. J. Coal Geol. **138** (6), 42, **2015**.

42. GANZ H., KALKREUTH W. Application of infrared spectroscopy to the classification of kerogentypes and the evaluation of source rock and oil shale potentials. Fuel, **66** (5), 708, **1987**.

43. ZODROW E.L., MASTALERZ M. Functional groups in a single pteridosperm species: variability and circumscription (Pennsylvanian, Nova Scotia, Canada). Int. J. Coal Geol. **70** (4), 313, **2007**.

44. NODA I. Generalized 2-dimensional correlation method applicable to infrared, raman, and other types of spectroscopy. Appl. Spectrosc. **47** (9), 1329, **1993**.

45. NODA I. Determination of two-dimensional correlation spectra using the hilbert transforms, Appl. Spectrosc. **54** (7), 994, **2000**.

46. MURAYAMA K., WU Y., CZARNIK-MATUSEWICZ B., OZAKI Y. Two-dimensional/attenuated total reflection infrared correlation spectroscopy studies on secondary structural changes in human serum albumin in aqueous solutions: pH-dependent structural changes in the secondary structures and in the hydrogen bondings of side chains. J. Phys. Chem. B. **105** (20), 4763, **2001**.

47. DING T., LU C.W., HE J., ZHAO B.Y., WANG J.H., HE E., ZHOU H.J., ZHANG Y. Adsorption characteristics of Pb^{2+} on natural black carbon extracted from different grain-size lake sediments. Environ. Sci. Pollut. Res. **23** (23), 23911, **2016**.

48. NADEEM R., MANZOOR Q., IQBAL M., NISAR J. Biosorption of Pb(II) onto immobilized and native Mangifera indica waste biomass. J. Ind. Eng. Chem. **35**, 185, **2016**.